

Least Restrictive Hyperplane Control Barrier Functions

Mattias Trende¹ and Petter Ögren¹

Abstract—Control Barrier Functions (CBFs) can provide provable safety guarantees for dynamic systems. However, finding a valid CBF for a system of interest is often non-trivial, especially if the shape of the unsafe region is complex and the CBFs are of higher order. A common solution to this problem is to make a conservative approximation of the unsafe region in the form of a line/hyperplane, and use the corresponding conservative Hyperplane-CBF when deciding on safe control actions. In this letter, we note that conservative constraints are only a problem if they prevent us from doing what we want. Thus, instead of first choosing a CBF and then choosing a safe control with respect to the CBF, we optimize over a combination of CBFs and safe controls to get as close as possible to our desired control, while still having the safety guarantee provided by the CBF. We call the corresponding CBF the least restrictive Hyperplane-CBF. Finally, we also provide a way of creating a smooth parameterization of the CBF-family for the optimization, and illustrate the approach on a double integrator dynamical system with acceleration constraints, moving through a group of arbitrarily shaped static and moving obstacles.

I. INTRODUCTION

Safety is crucial for dynamic systems, whether they are fully autonomous or include humans-in-the-loop. Over the last two decades, Control Barrier Functions (CBFs) have gained popularity as a means to ensure safety [1]–[3]. The role of a CBF is typically to serve as a safety filter. Given the state, the CBF can give you a set of safe control actions, and given a desired control action and a CBF, you can determine the safe control action that is closest to the desired one.

The difficult part of using CBFs to ensure safety is often to find a valid CBF [4]. For low-dimensional systems with simple obstacle geometries, it is often possible to derive a CBF analytically [5], but for more complex geometries and higher-dimensional systems, a closed-form solution might not be available, and numerical solutions scale poorly with the increasing complexity [4]. A common solution to this problem is to utilize some type of approximate CBF. There are machine learning approaches to the problem [6], but using a black box model to guarantee safety can create additional challenges. Another common approach is to use over-approximating hyperplanes to create the CBF [7]–[11].

By using a Hyperplane-CBF (H-CBF), the problem dimensionality is essentially reduced by projecting the system’s movement orthogonally to the plane [7]. This enables the use of an analytically derived one-dimensional CBF for higher-dimensional systems, while keeping the safety guarantees.

¹The authors are with the Robotics, Perception and Learning Lab, School of Electrical Engineering and Computer Science, Royal Institute of Technology (KTH), SE-100 44 Stockholm, Sweden, {mtrende, petter}@kth.se

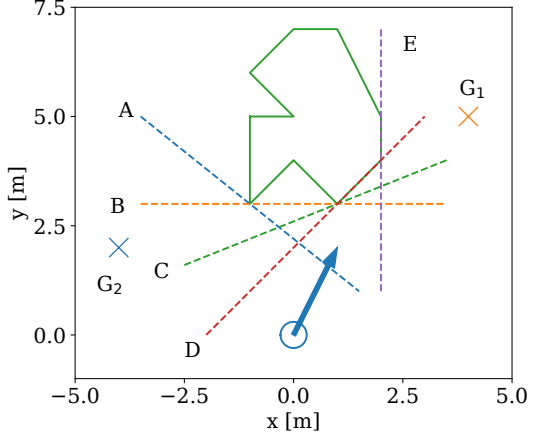


Fig. 1. A robot at position $(0, 0)$ with velocity $(1, 2)$ in front of a polygonal obstacle. Five of the infinitely many supporting hyperplanes, parameterized by some θ , are shown (A-E). If the goal is at G_1 , an H-CBF based on D is the least restrictive, whereas if the goal is at G_2 , an H-CBF based on A or B might be the least restrictive. Thus, we propose to optimize over θ at the same time as the control u , to find the least restrictive H-CBF.

This approach also enables over-approximation of a multitude of obstacle geometries, including circles, ellipses, and polygons [7], [10], [12]. However, the downside of the H-CBF is that it is often quite conservative. However, in this letter we note that a conservative CBF is only a problem if it prevents us from doing what we want. Thus, we propose to find *the least restrictive H-CBF* as follows.

We first parameterize the family of H-CBFs for a given obstacle with some parameter θ . Then, given some desired control u_{des} , we jointly optimize over the control action u and θ such that u is safe with respect to θ and the distance $\|u - u_{\text{des}}\|$ is minimized. This yields the least restrictive H-CBF and the most suitable corresponding safe control action. An illustration of this is provided in Figure 1. The dashed lines represent different choices of θ , and the one denoted D represents the least restrictive H-CBF, when aiming for the rightmost goal location G_1 .

Note that in the standard CBF approach [4], the optimization problem above (without θ) is called a CBF-QP, since if the system is control affine, $\dot{x} = f(x) + g(x)u$, the optimization is a quadratic programming (QP) problem which is very easy to solve numerically. Including θ in the optimization, we get a non-convex optimization problem that might be harder to solve. To address this problem, we present a way to create a smooth parameterization of the H-CBFs, allowing fast numerical solutions. While a new solution for u is needed every timestep for the safety guarantees, we

also note that θ can be updated less frequently, based on the available computation resources. The old θ still guarantees safety, and updating θ only influences how conservative the chosen H-CBF is, see Remark 1.

Thus, the main contribution of this letter is a method to optimize the choice of H-CBF simultaneously with the choice of the control action, thereby minimizing the difference between the chosen safe control and the desired control. We also propose a way to parameterize the family of possible H-CBFs and show how the result is less restrictive than the commonly used orthogonal H-CBFs [7].

In the remainder of this letter, Section II looks further into the connections to previous work, while Section III summarizes the theory of CBFs as well as the double integrator model with a corresponding H-CBF. Then, Section IV describes the proposed approach. Finally, the results from the simulations are presented in Section V, and the letter is concluded in Section VI.

II. RELATED WORK

There has been a lot of work on CBFs connected to different ways of approximating obstacles. The four most common ways are circles [7], [8], ellipses [10], [13], polygons [14]–[18], and hyperplanes [7], [8], [10], [12], [19]–[21]. In the last category, we also include the common CBF approach that keeps track of the distance from the robot to the closest point on an obstacle and makes sure this distance is kept positive [7], [19], [21]. Note that even though this approach does not explicitly mention hyperplanes, it is equivalent to an H-CBF touching the closest point of the obstacle, with a normal vector pointing towards the robot. Throughout the letter, we refer to these H-CBFs as *orthogonal*, as they are orthogonal to the line between the robot and the closest point on the obstacle.

There are also other works suggesting different orientations of H-CBFs. In [10], ellipsoidal bodies are considered, and the orientation of the hyperplane is chosen to maximize the distance between the hyperplane and the other nearby ellipsoid. In [20], the orientation of the H-CBF was chosen based on velocity obstacles (VO). They consider a second-order dynamic system, but in order to avoid having to work with higher-order CBFs, they create the CBFs in velocity space, aligned with the VO. Finally, [12] picks H-CBFs based on a safe convex polytope, generated from free space in an occupancy grid map.

In this letter, the parameterization of the family of H-CBFs connected to each obstacle was inspired by a description that was originally used for artificial potential fields [22], and then repurposed for CBFs [17], [23]. However, the proposed approach in this letter does not perform any map transformations.

We also note that our use of H-CBFs makes the proposed approach suitable for combinations with several other methods in the literature, such as work on multi-agent systems [8], [24], [25], cooperative/neutral/adversarial obstacles [7], [26] and MPC [13], [27].

Finally, we note that this letter is different from all the approaches mentioned above in the sense that it includes the choice of H-CBF in the optimization of the chosen control. Thus, it finds the least restrictive H-CBF, in terms of finding a safe control as close as possible to the desired control. All other papers first choose a CBF, then choose a safe control. We believe that there are advantages to doing both choices at the same time. ■

III. BACKGROUND

In this section, we first review some results from convex analysis, then summarize CBF theory, followed by a description of double integrator models and how we can create an H-CBF for them.

A. Convex Analysis

Definition 1: A supporting hyperplane to a set $S \subset \mathbb{R}^n$ at a point $\mathbf{x}_0 \in \partial S$ (the boundary of S) is a hyperplane that: passes through the point \mathbf{x}_0 and leaves the entire set on one side of the hyperplane (or on the hyperplane itself).

Theorem 1 (Supporting Hyperplane in Every Direction): If a set $S \subset \mathbb{R}^n$ is closed, convex, bounded, and has nonempty interior, then for every nonzero direction $\mathbf{r} \in \mathbb{R}^n$ there exists a point $\mathbf{x}^* \in S$ such that

$$\mathbf{r}^T \mathbf{x}^* = \sup_{\mathbf{x} \in S} \mathbf{r}^T \mathbf{x} \quad (1)$$

and the hyperplane $\{\mathbf{x} : \mathbf{r}^T \mathbf{x} = \mathbf{r}^T \mathbf{x}^*\}$ supports S at \mathbf{x}^* . ■

Proof: See [28]. ■

Theorem 2 (Separating Hyperplane): Let $C_1, C_2 \subset \mathbb{R}^n$ be two compact, convex, nonempty, disjoint sets. Then, there exists a separating hyperplane $\mathbf{a}^T \mathbf{x} = b$, such that

$$\mathbf{a}^T \mathbf{x} \leq b \quad \forall \mathbf{x} \in C_1 \quad (2)$$

$$\mathbf{a}^T \mathbf{x} \geq b \quad \forall \mathbf{x} \in C_2. \quad (3)$$

Proof: See [28]. ■

B. Control Barrier Functions

Following the CBF definition in [3], consider a nonlinear affine control system in the form of

$$\dot{\mathbf{x}} = \mathbf{f}(\mathbf{x}) + \mathbf{g}(\mathbf{x})\mathbf{u}, \quad (4)$$

where \mathbf{f} and \mathbf{g} are locally Lipschitz, $\mathbf{x} \in \mathbb{R}^n$ is the system state, and $\mathbf{u} \in \mathbb{R}^m$ is the system input. Then introduce the safe set \mathcal{C} , defined such that for every state $\mathbf{x}(t) \in \mathcal{C}$ there exists a permissible control $\mathbf{u} \in \mathcal{U}$ that ensures $\mathbf{x}(t + \epsilon) \in \mathcal{C}$ for all $\epsilon > 0$. Consider a continuously differentiable function $h : \mathbb{R}^n \rightarrow \mathbb{R}$. If h then follows

$$h(\mathbf{x}) \geq 0 \quad \forall \mathbf{x} \in \mathcal{C}, \quad (5)$$

$$h(\mathbf{x}) = 0 \quad \forall \mathbf{x} \in \partial \mathcal{C}, \quad (6)$$

$$h(\mathbf{x}) < 0 \quad \forall \mathbf{x} \notin \mathcal{C}, \quad (7)$$

and satisfies the inequality

$$\sup_{\mathbf{u}} \dot{h}(\mathbf{x}, \mathbf{u}) \geq -\alpha(h(\mathbf{x})), \quad (8)$$

then h is a CBF. Here $\alpha : \mathbb{R} \rightarrow \mathbb{R}$ is an extended class \mathcal{K}_∞ function. This defines α to be a strictly increasing function that satisfies $\alpha(0) = 0$ and $\lim_{x \rightarrow \pm\infty} \alpha(x) = \pm\infty$.

To use a CBF to ensure safety, the first step is to pick a starting state within \mathcal{C} , equivalent to $h(\mathbf{x}) \geq 0$. The key idea is then to keep track of h , ensuring it never goes negative. This is ensured by the condition (8). Given a desired control \mathbf{u}_{des} the search of a safe control \mathbf{u} close to the desired one can be formalized in the following optimization problem [3]:

Problem 1 (CBF-QP):

$$\mathbf{u}(\mathbf{x}) = \underset{\mathbf{u}}{\operatorname{argmin}} \ (\mathbf{u} - \mathbf{u}_{\text{des}})^T \mathbf{Q} (\mathbf{u} - \mathbf{u}_{\text{des}}) \quad (9)$$

$$\text{s.t. } \dot{h}(\mathbf{x}) \geq -\alpha(h(\mathbf{x})) \quad (10)$$

$$\mathbf{u} \in \mathcal{U}. \quad (11)$$

Here Q is a positive definite matrix and \mathcal{U} is the set of available controls.

It can be shown that if the dynamics are given by (4), the problem above is a Quadratic Programming problem (QP) that is easy to solve.

C. Double Integrator Model

In this letter, we will consider a double integrator dynamic model with acceleration constraints. Let the state be $\mathbf{x} = (\mathbf{p}, \mathbf{v}) \in \mathbb{R}^4$ and

$$\begin{aligned} \dot{\mathbf{p}} &= \mathbf{v} \\ \dot{\mathbf{v}} &= \mathbf{u} \end{aligned} \quad (12)$$

with the acceleration constraint $\|\mathbf{u}\| \leq u_{\text{max}}$. Then (12) can be written in control-affine form

$$\dot{\mathbf{x}} = \mathbf{f}(\mathbf{x})\mathbf{x} + \mathbf{g}(\mathbf{x})\mathbf{u} = \mathbf{A}\mathbf{x} + \mathbf{B}\mathbf{u}, \quad (13)$$

where \mathbf{A} and \mathbf{B} are given by,

$$\mathbf{A} = \begin{bmatrix} 0 & 0 & 1 & 0 \\ 0 & 0 & 0 & 1 \\ 0 & 0 & 0 & 0 \\ 0 & 0 & 0 & 0 \end{bmatrix}, \quad \mathbf{B} = \begin{bmatrix} 0 & 0 \\ 0 & 0 \\ 1 & 0 \\ 0 & 1 \end{bmatrix}. \quad (14)$$

D. An H-CBF for the Double Integrator

For the dynamic model in (12), a H-CBF for an agent $(\mathbf{p}_i, \mathbf{v}_i)$ and an obstacle $(\mathbf{p}_j, \mathbf{v}_j)$ is given by [7]

$$h_{ij}(\mathbf{x}_i) = \hat{\mathbf{n}}_{ij}^T(\mathbf{p}_i - \mathbf{p}_j) - \delta_{ij} - b_{ij}(\mathbf{x}_i). \quad (15)$$

Here $\hat{\mathbf{n}}_{ij}$ is a unit vector pointing in the direction from \mathbf{p}_j towards \mathbf{p}_i , δ_{ij} is the required safety margin between agent and the obstacle, and b_{ij} is the braking distance needed for the agent to accelerate to the relative velocity of zero compared to the obstacle. The braking distance is given by

$$b_{ij}(\mathbf{x}_i) = \begin{cases} \frac{(\hat{\mathbf{n}}_{ij}^T(\mathbf{v}_i - \mathbf{v}_j))^2}{2u_{\text{max}}}, & \text{for } \hat{\mathbf{n}}_{ij}^T(\mathbf{v}_i - \mathbf{v}_j) < 0 \\ 0, & \text{for } \hat{\mathbf{n}}_{ij}^T(\mathbf{v}_i - \mathbf{v}_j) \geq 0 \end{cases}, \quad (16)$$

since no braking is needed when the agent and obstacle are moving away from each other.

IV. PROPOSED APPROACH

The key idea of the proposed approach is to replace a given CBF $h(\mathbf{x})$ by a family of CBFs $h(\mathbf{x}, \theta)$ parameterized by θ , and optimize jointly over the control \mathbf{u} and the CBF parameter θ . Thus, we replace Problem 1 (CBF-QP) with the parameterized P-CBF-QP.

Problem 2 (P-CBF-QP):

$$\mathbf{u}(\mathbf{x}) = \underset{\mathbf{u}, \theta}{\operatorname{argmin}} \ (\mathbf{u} - \mathbf{u}_{\text{des}})^T \mathbf{Q} (\mathbf{u} - \mathbf{u}_{\text{des}}) \quad (17)$$

$$\text{s.t. } \dot{h}(\mathbf{x}, \theta) \geq -\alpha(h(\mathbf{x}, \theta)) \quad (18)$$

$$h(\mathbf{x}, \theta) \geq 0 \quad (19)$$

$$\mathbf{u} \in \mathcal{U}. \quad (20)$$

Note that we have added line (19) to make sure that the chosen CBF is such that \mathbf{x} is still feasible.

Now this approach can, in principle, be applied to any family of CBFs, but we have chosen H-CBFs since they have closed-form solutions for second-order systems like (12), and the degree of conservativeness depends a lot on their orientation. To create the parameterized family of H-CBFs $h(\mathbf{x}, \theta)$, we make use of the following lemma.

Lemma 1: Given a compact obstacle $\mathcal{O} \subset \mathbb{R}^n$ with non-empty interior and a vector $\hat{\mathbf{n}}(\theta)$, there is a H-CBF $h(\mathbf{x}, \theta)$ with normal $\hat{\mathbf{n}}(\theta)$ that is a supporting hyperplane to $\text{conv}(\mathcal{O})$, the convex hull of the obstacle.

Proof: $\text{conv}(\mathcal{O})$ is closed, convex, bounded, and has nonempty interior. By Theorem 1 there is a supporting hyperplane with normal $\hat{\mathbf{n}}(\theta)$ that can be turned into a H-CBF $h(\mathbf{x}, \theta)$ using (15) and (16). ■

As noted above, we are using the freedom in choosing θ to reduce the conservativeness of H-CBFs. To get an additional feeling for which extent this is possible, we present the following result.

Lemma 2: Given an obstacle $\mathcal{O}_i \subset \mathbb{R}^n$, and a robot trajectory $P = \{p_1, p_2, \dots\} \subset \mathbb{R}^n$ ending at stand still. If the convex hull of the obstacle and the convex hull of the trajectory positions do not intersect, i.e., $\text{conv}(\mathcal{O}_i) \cap \text{conv}(P) = \emptyset$, then there exists a choice θ and α such that the H-CBF $h(\mathbf{x}, \theta)$ would have guaranteed the safety of P .

Proof: By Theorem 2, there exists a hyperplane separating the obstacle from the trajectory. Since the trajectory ends at a standstill and never intersects the hyperplane, the agent's velocity is always safe from a hyperplane collision point of view. By choosing α large enough, the trajectory will satisfy the CBF condition (18). ■

Finally, we note that the H-CBFs for double integrators in Section III-D provide guarantees for both static ($\mathbf{v}_j = 0$) and moving ($\mathbf{v}_j \neq 0$) obstacles. Thus, both cases can be handled, see Figure 8 below.

In the remainder of this section, we discuss different parameterizations of the H-CBF $h(\mathbf{x}, \theta)$. First, we cover the simplest case of disc-shaped obstacles, then the general case, followed by ellipses.

A. Disc Worlds

To parameterize the H-CBF using θ , the orthogonal unit vector $\hat{\mathbf{n}}_{ij}$ in (15) is replaced with the θ dependent unit vector

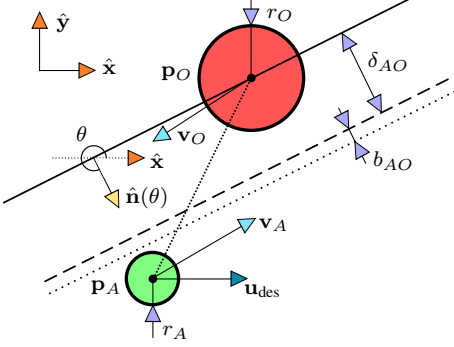


Fig. 2. The geometry of the simple disc world. The green circle represents the agent (A), and the red circle represents the obstacle (O). Many of the vectors used to define the CBF hyperplane are shown as arrows.

$\hat{\mathbf{n}}(\theta) = [\cos(\theta), \sin(\theta)]^T$. An overview of the geometry is presented in Figure 2. Applying Equations (15) and (16), we get the following θ -dependent H-CBF, protecting agent i from obstacle j .

$$h_{ij}(\mathbf{x}_i, \theta) = \hat{\mathbf{n}}(\theta)^T(\mathbf{p}_i - \mathbf{p}_j) - \delta_{ij} - b_{ij}, \quad (21)$$

where

$$b_{ij} = \begin{cases} \frac{(\hat{\mathbf{n}}(\theta)^T \mathbf{v}_{ij})^2}{2u_{\max}}, & \text{for } \hat{\mathbf{n}}(\theta)^T(\mathbf{v}_i - \mathbf{v}_j) < 0 \\ 0, & \text{for } \hat{\mathbf{n}}(\theta)^T(\mathbf{v}_i - \mathbf{v}_j) \geq 0 \end{cases}. \quad (22)$$

To calculate the derivative of h with respect to time, as needed in (18), consider the case in which $b_{ij} \neq 0$. It then follows that

$$\begin{aligned} \dot{h}_{ij}(\mathbf{x}_i, \theta) &= \nabla h_{ij}(\mathbf{x}_i, \theta) \dot{\mathbf{x}}_i \\ &= \hat{\mathbf{n}}(\theta)^T(\mathbf{v}_i - \mathbf{v}_j - \mathbf{u}_i) \frac{\hat{\mathbf{n}}(\theta)^T(\mathbf{v}_i - \mathbf{v}_j)}{u_{\max}}. \end{aligned} \quad (23)$$

Remark 1: When inserting (21) and (23) into (18), we get a possibly non-convex function with respect to θ . Thus, Problem 2 is only a QP for fixed θ , and a general numerical solver such as CasADi [29] is needed when jointly optimizing over θ and \mathbf{u} . However, note that the θ from the previous time step is always a feasible option, so if computational resources are scarce, the fixed- θ QP can be solved every timestep, and the optimization including θ can be done on a slower time-scale.

B. General (Nonconvex) Obstacles

Consider a generally shaped obstacle \mathcal{O} , as in Figure 3. The convex hull of the obstacle is denoted $\text{conv}(\mathcal{O})$, and due to convexity, we can describe the perimeter of $\text{conv}(\mathcal{O})$ as

$$\partial\text{conv}(\mathcal{O}) = \{\mathbf{x} | \mathbf{x} = \mathbf{p}_o + \hat{\mathbf{n}}(\phi)r(\phi), \phi \in [0, 2\pi)\} \quad (24)$$

where $\mathbf{p}_o \in \text{conv}(\mathcal{O})$, and $r : \mathbb{R} \rightarrow \mathbb{R}$ is the radial distance.

With this representation, we can introduce the angle-dependent safety distance function $\delta_j(\theta)$ as

$$\delta_j(\theta) = \max_{\phi} \{\hat{\mathbf{n}}(\theta)^T \hat{\mathbf{n}}(\phi)r(\phi)\}. \quad (25)$$

This describes the maximum distance that $\text{conv}(\mathcal{O})$ extends out from the halfplane crossing \mathbf{p}_o with the normal vector

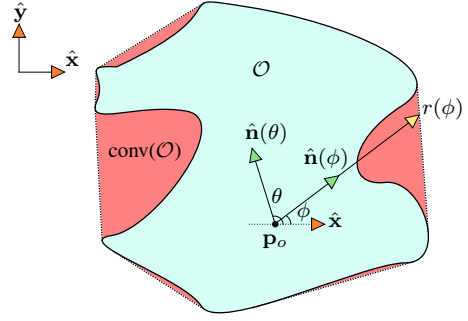


Fig. 3. The geometries of a general 2D obstacle. The light blue area is the obstacle \mathcal{O} , and combined with the red areas, we get $\text{conv}(\mathcal{O})$.

$\hat{\mathbf{n}}(\theta)$. Then, the total safety distance needed between the center of the circular agent i (radius r_i) and the obstacle point \mathbf{p}_j as a function of θ is given by

$$\delta_{ij}(\theta) = r_i + \delta_j(\theta). \quad (26)$$

Inserting (26) into (21), we get the parameterized H-CBF for any obstacle. Note that the optimization in (26) only needs to be done once for each obstacle.

For a general function $r(\phi)$ in (25), it is often impossible to express $\delta_{ij}(\theta)$ in (21) in a closed form that can be used in Problem 2. In these cases, we instead suggest computing a smooth approximation $\tilde{\delta}_j(\theta)$ using a Fourier series.

First, we discretize θ , and for each discrete θ , perform the optimization (25). Then we have a discrete set of $\delta_j(\theta)$. We approximate these with a Fourier series, truncated to some suitable number of terms N_j . This gives

$$\tilde{\delta}_j(\theta) \approx \frac{a_0}{2} + \sum_{n=1}^{N_j} (a_n \cos(n\theta) + b_n \sin(n\theta)). \quad (27)$$

To ensure that this approximation is conservative (not violating the safety guarantees), an additional safety margin δ_j^m can be added. The minimal margin is given by

$$\delta_j^m = \max_{\theta} \delta_j(\theta) - \tilde{\delta}_j(\theta), \quad (28)$$

and this finally results in the smooth, but approximate, radial safety distance function

$$\delta_{ij}(\theta) = r_i + \tilde{\delta}_j(\theta) + \delta_j^m. \quad (29)$$

C. Elliptical Obstacles

For elliptically shaped obstacles, it is possible to calculate (25) analytically as follows.

Lemma 3: For an ellipse given in the form

$$\mathbf{r}(\gamma) = \begin{bmatrix} a \cos(\gamma) \\ b \sin(\gamma) \end{bmatrix}, \quad (30)$$

where a is the major axis, b is the minor axis, and the angle γ is called the eccentric anomaly, the optimization problem in (25) has the solution

$$\delta_j(\theta) = a \cos(\theta) \cos(\gamma_{\max}) + b \sin(\theta) \sin(\gamma_{\max}), \quad (31)$$

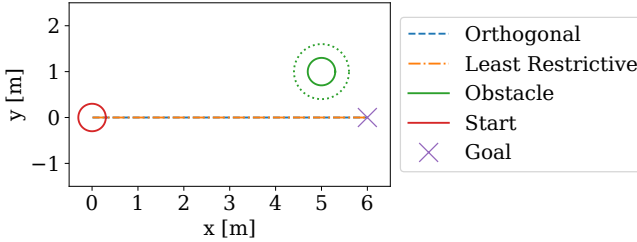


Fig. 4. The setup of example 1. The agent moves on a straight line, safely passing an obstacle. The corresponding value of the CBF constraint (18) for the two different cases is shown in Figure 5.

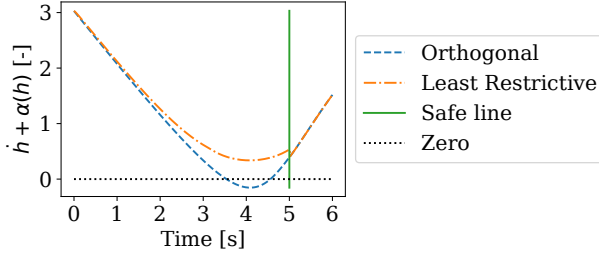


Fig. 5. The CBF constraint (18) with $\alpha(x) = x$ for the agent in Example 1. Note that this safe trajectory would not be allowed by the orthogonal CBF of [7] (dashed), as it is negative for $t \in [3.5, 4.5]$, right before passing the obstacle. However, it would be allowed by the least restrictive H-CBF (dash-dotted). Note that the two CBFs are identical when the agent is moving away from the obstacle, after passing the “safe line” at $t = 5$ s, since then $b_{ij} = 0$ for both, see Equation (16).

where $\gamma_{\max} = \arctan 2(b \sin(\theta), a \cos(\theta))$.

Proof: Inserting (30) into (25), we get

$$\delta_j(\theta) = \max_{\gamma} \{\hat{\mathbf{n}}(\theta)^T \mathbf{r}(\gamma)\}. \quad (32)$$

Setting the derivative to zero gives

$$\frac{\partial}{\partial \gamma} (\hat{\mathbf{n}}(\theta)^T \mathbf{r}(\gamma)) = -\cos(\theta) a \sin(\gamma) + \sin(\theta) b \cos(\gamma) = 0 \quad (33)$$

which in turn gives the γ_{\max} above, corresponding to (31). \blacksquare

The result can be extended to an arbitrary ellipse rotated by an angle β .

V. SIMULATIONS

In this section, the proposed approach is illustrated in three examples with increasing complexity, using a 2D double integrator. We compare the least restrictive H-CBF with the orthogonal H-CBF from [7]. The simulations are conducted in Python, and the joint optimization over θ and \mathbf{u} is solved with CasADi [29].

Example 1: In the first example, the agent moves on a straight line, safely passing a static obstacle, as seen in Figure 4. This path is, however, not feasible with respect to an orthogonal H-CBF, as seen in Figure 5. This shows that the optimization over θ is indeed less restrictive.

Example 2: In the second example, the orthogonal and least restrictive H-CBFs are compared to each other in a

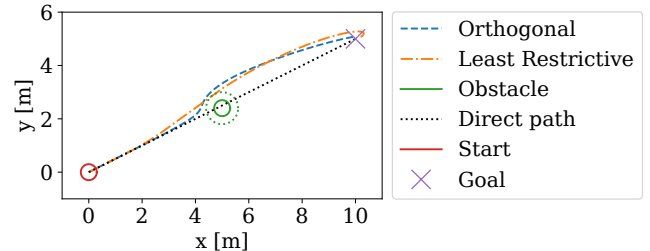


Fig. 6. The setup of example 2. The agent is driven towards the goal with a PD-controller, using the two types of H-CBFs. Note how the least restrictive H-CBF leaves the dotted straight line path early with a small correction of the path, while the orthogonal H-CBF results in a significant slowdown, and turn closer to the obstacle. As can be seen in Figure 7 the orthogonal H-CBF actually starts slowing down before the least restrictive starts turning. This is expected, as it is searching for a θ to minimize $\|\mathbf{u} - \mathbf{u}_{\text{des}}\|$.

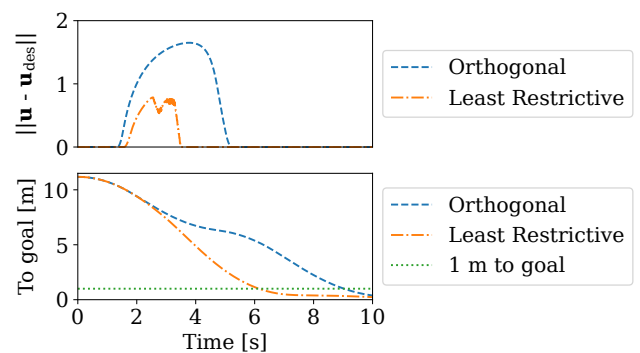


Fig. 7. Upper: The difference between the desired control and the safe control $\|\mathbf{u} - \mathbf{u}_{\text{des}}\|$ over time. The orthogonal H-CBF comes into effect earlier and for a longer time, compared to the least restrictive H-CBF. Lower: The distance to the goal as a function of time. The orthogonal H-CBF arrives within 1 m of the goal in 9.0 s, while the least restrictive H-CBF does so in 6.1 s.

scenario with a single static obstacle blocking the direct path to the goal, as seen in Figure 6, with corresponding data in Figure 7. The agent starts at rest and is driven by a PD-controller that provides \mathbf{u}_{des} . As can be seen from $\|\mathbf{u} - \mathbf{u}_{\text{des}}\|$ in Figure 7 (upper), the orthogonal H-CBF starts to restrict acceleration earlier than the least restrictive H-CBF, enforces a larger gap $\|\mathbf{u} - \mathbf{u}_{\text{des}}\|$, and does so for a longer time. Furthermore, looking at the trails of the paths in Figure 6, we see that the orthogonal H-CBF stays on the dotted straight line path longer while slowing down, and starts turning fairly late, while the least restrictive H-CBF leaves the dotted path earlier, maintains a higher speed (slope of goal distance plot), and arrives at the goal much sooner.

Example 3: In the third example, the agent encounters two static polygon-shaped obstacles, as well as an ellipse moving at constant velocity. The results for both the orthogonal and the least restrictive CBF halfplanes are shown in Figure 8. Notice how the optimized halfplanes enable the agent to move closer to the obstacles, and at a greater velocity compared to the orthogonal halfplanes.

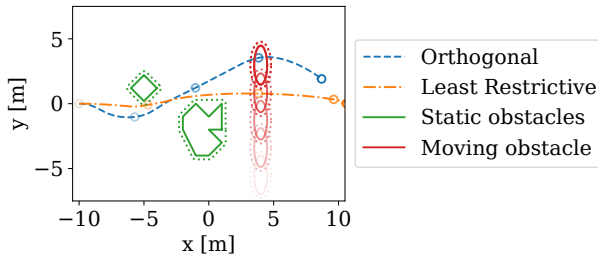


Fig. 8. The trajectories in example 3, featuring moving and irregularly shaped obstacles. Concurrent snapshots of the agent and the moving obstacle are shown, with older ones increasingly opaque. Notice how the least restrictive approach is less conservative in regards to the obstacles, resulting in a faster trajectory.

VI. CONCLUSION

In all earlier work, the CBF is chosen before it is time to find a safe control. In this letter, we suggest making the two choices at the same time, to make sure we find the least restrictive CBF, in relation to what we want to do. The advantages of the proposed approach were illustrated in three examples, including moving obstacles. In future work, we intend to apply the approach to real autonomous systems, exploring how one can extend the approach beyond the double integrator model, and how often the optimization with respect to θ can be performed, given available computational resources.

REFERENCES

- [1] S. Prajna, A. Jadbabaie, and G. J. Pappas, “A Framework for Worst-Case and Stochastic Safety Verification Using Barrier Certificates,” *IEEE Transactions on Automatic Control*, vol. 52, no. 8, pp. 1415–1428, Aug. 2007.
- [2] A. D. Ames, J. W. Grizzle, and P. Tabuada, “Control barrier function based quadratic programs with application to adaptive cruise control,” in *53rd IEEE Conference on Decision and Control*, Dec. 2014, pp. 6271–6278, iSSN: 0191-2216.
- [3] A. D. Ames, S. Coogan, M. Egerstedt, G. Notomista, K. Sreenath, and P. Tabuada, “Control Barrier Functions: Theory and Applications,” in *2019 18th European Control Conference (ECC)*, Jun. 2019, pp. 3420–3431.
- [4] K.-C. Hsu, H. Hu, and J. F. Fisac, “The Safety Filter: A Unified View of Safety-Critical Control in Autonomous Systems,” *Annual Review of Control, Robotics, and Autonomous Systems*, vol. 7, no. 1, pp. 47–72, Jul. 2024.
- [5] Y. Chen, M. Jankovic, M. Santillo, and A. D. Ames, “Backup Control Barrier Functions: Formulation and Comparative Study,” Apr. 2021, arXiv:2104.11332 [eess].
- [6] H. Yu, C. Hirayama, C. Yu, S. Herbert, and S. Gao, “Sequential Neural Barriers for Scalable Dynamic Obstacle Avoidance,” in *2023 IEEE/RSJ International Conference on Intelligent Robots and Systems (IROS)*, Oct. 2023, pp. 11 241–11 248, iSSN: 2153-0866.
- [7] U. Borrmann, L. Wang, A. D. Ames, and M. Egerstedt, “Control Barrier Certificates for Safe Swarm Behavior,” *IFAC-PapersOnLine*, vol. 48, no. 27, pp. 68–73, Jan. 2015.
- [8] L. Wang, A. D. Ames, and M. Egerstedt, “Safety Barrier Certificates for Collisions-Free Multirobot Systems,” *IEEE Transactions on Robotics*, vol. 33, no. 3, pp. 661–674, Jun. 2017.
- [9] T. G. Molnar, S. K. Kannan, J. Cunningham, K. Dunlap, K. L. Hobbs, and A. D. Ames, “Collision Avoidance and Geofencing for Fixed-Wing Aircraft With Control Barrier Functions,” *IEEE Transactions on Control Systems Technology*, vol. 33, no. 5, pp. 1493–1508, Sep. 2025.
- [10] R. Funada, K. Nishimoto, T. Ibuki, and M. Sampei, “Collision Avoidance for Ellipsoidal Rigid Bodies With Control Barrier Functions Designed From Rotating Supporting Hyperplanes,” *IEEE Transactions on Control Systems Technology*, vol. 33, no. 1, pp. 148–164, Jan. 2025.
- [11] E. H. Thyri, E. A. Basso, M. Breivik, K. Y. Pettersen, R. Skjetne, and A. M. Lekkas, “Reactive collision avoidance for ASVs based on control barrier functions,” in *2020 IEEE Conference on Control Technology and Applications (CCTA)*, Aug. 2020, pp. 380–387.
- [12] S. Liu, Y. Mao, and C. A. Belta, “Safety-Critical Planning and Control for Dynamic Obstacle Avoidance Using Control Barrier Functions,” in *2025 American Control Conference (ACC)*, Jul. 2025, pp. 348–354, iSSN: 2378-5861.
- [13] P. Tooranjiipour and B. Kiumarsi, “LiDAR-based Model Predictive Control using Control Barrier Functions,” in *2025 American Control Conference (ACC)*, Jul. 2025, pp. 315–322, iSSN: 2378-5861.
- [14] A. Thirugnanam, J. Zeng, and K. Sreenath, “Safety-Critical Control and Planning for Obstacle Avoidance between Polytopes with Control Barrier Functions,” in *2022 International Conference on Robotics and Automation (ICRA)*, May 2022, pp. 286–292.
- [15] S. Wu, Y. Fang, N. Sun, B. Lu, X. Liang, and Y. Zhao, “Optimization-Free Smooth Control Barrier Function for Polygonal Collision Avoidance,” *IEEE Transactions on Cybernetics*, vol. 55, no. 9, pp. 4257–4269, Sep. 2025.
- [16] S. Wei, R. Khorrambakh, P. Krishnamurthy, V. Mariano Gonçalves, and F. Khorrami, “Collision Avoidance for Convex Primitives via Differentiable Optimization-Based High-Order Control Barrier Functions,” *IEEE Transactions on Control Systems Technology*, pp. 1–16, 2025.
- [17] G. Notomista, G. P. T. Choi, and M. Saveriano, “Reactive Robot Navigation Using Quasi-Conformal Mappings and Control Barrier Functions,” *IEEE Transactions on Control Systems Technology*, vol. 33, no. 3, pp. 928–939, May 2025.
- [18] B. Dai, R. Khorrambakh, P. Krishnamurthy, V. Gonçalves, A. Tzes, and F. Khorrami, “Safe Navigation and Obstacle Avoidance Using Differentiable Optimization Based Control Barrier Functions,” *IEEE Robotics and Automation Letters*, vol. 8, no. 9, pp. 5376–5383, Sep. 2023, arXiv:2304.08586 [cs].
- [19] A. Ghaffari, I. Abel, D. Ricketts, S. Lerner, and M. Krstic, “Safety Verification Using Barrier Certificates with Application to Double Integrator with Input Saturation and Zero-Order Hold,” in *2018 Annual American Control Conference (ACC)*. Milwaukee, WI: IEEE, Jun. 2018, pp. 4664–4669.
- [20] J. Huang, J. Zeng, X. Chi, K. Sreenath, Z. Liu, and H. Su, “Dynamic Collision Avoidance Using Velocity Obstacle-Based Control Barrier Functions,” *IEEE Transactions on Control Systems Technology*, vol. 33, no. 5, pp. 1601–1615, Sep. 2025.
- [21] A. S. Roncero, R. I. C. Muchacho, and P. Ögren, “Multi-Agent Obstacle Avoidance using Velocity Obstacles and Control Barrier Functions,” Mar. 2025, arXiv:2409.10117 [cs].
- [22] E. Rimon and D. E. Koditschek, “The construction of analytic diffeomorphisms for exact robot navigation on star worlds,” *Transactions of the American Mathematical Society*, vol. 327, no. 1, pp. 71–116, 1991.
- [23] G. Notomista and M. Saveriano, “Safety of Dynamical Systems With Multiple Non-Convex Unsafe Sets Using Control Barrier Functions,” *IEEE Control Systems Letters*, vol. 6, pp. 1136–1141, 2022.
- [24] L. An and G.-H. Yang, “Collisions-Free Distributed Optimal Coordination for Multiple Euler-Lagrangian Systems,” *IEEE Transactions on Automatic Control*, vol. 67, no. 1, pp. 460–467, Jan. 2022.
- [25] X. Tan and D. V. Dimarogonas, “Distributed Implementation of Control Barrier Functions for Multi-agent Systems,” *IEEE Control Systems Letters*, vol. 6, pp. 1879–1884, 2022.
- [26] D. Martínez-Baselga, E. Sebastián, E. Montijano, L. Riazuelo, C. Sagüés, and L. Montano, “AVOCADO: Adaptive Optimal Collision Avoidance Driven by Opinion,” *IEEE Transactions on Robotics*, vol. 41, pp. 2495–2511, 2025.
- [27] M. A. Abbas, R. Milman, and J. M. Eklund, “Obstacle Avoidance in Real Time With Nonlinear Model Predictive Control of Autonomous Vehicles,” *Canadian Journal of Electrical and Computer Engineering*, vol. 40, no. 1, pp. 12–22, 2017.
- [28] T. Rockafellar, *Convex Analysis*. Princeton University Press, 1970.
- [29] J. A. E. Andersson, J. Gillis, G. Horn, J. B. Rawlings, and M. Diehl, “CasADi: a software framework for nonlinear optimization and optimal control,” *Mathematical Programming Computation*, vol. 11, no. 1, pp. 1–36, Mar. 2019.